Spatial effects on electrospray ionization response

Eric Janusson, Amelia V. Hesketh, Karlee L. Bamford, Katherine Hatlelid, Rehan Higgins, J. Scott McIndoe*

Department of Chemistry, University of Victoria, P.O. Box 3065, Victoria, BC V8W3V6, Canada

ARTICLE INFO

ABSTRACT

The position of the spray-head, the solvent, and a variety of additional instrumental parameters were independently adjusted during electrospray ionization mass spectrometric (ESI-MS) analysis of an equimolar mixture of two different ions. These parameters were found to have drastic effects on the distribution of signal intensity from one ion to another, and therefore the resulting usefulness of acquired spectra. The analytes studied were bis(triphenylphosphine)iminium (PPN) chloride and tetramethylammonium (TMA) chloride, two chemically distinct ions. The use of these two ions in a test solution yielded information regarding ESI probe spatial effects for two very different analytes, while probing the issue of sampling efficiency. Each experimental parameter was individually adjusted prior to rastering the spray head across the operational plane in order to observe how adjustment to a particular parameter affects analyte signal in relation to the distance from the MS aperture. Following acquisition, the intensities of both ions were plotted as ion contour maps demonstrating the intensity change with respect to capillary position in relation to the mass spectrometer aperture. The sharp contrast in ion intensity, and even differential ion activity, with relatively minor instrument changes (such as temperature programming, gas flow rates and solvent choice) clearly demonstrates the importance of finding the "sweet spot" for the ESI spray head, especially when signal intensity and a quality analysis are key.

1. Introduction

The electrospray process is complex enough that following several decades of widespread use, the exact mechanism of producing gas phase ions from condensed phase analytes in solution continues to be scrutinized. Adding to the complexity of the electrospray process is the development of varied source designs and geometries. Common designs include the TurboV from MDS SCIEX, the Ion Max from Thermo, along with the Waters/Micromass Z-Spray source design, which is dealt with in the present work (see figure S14 in the supporting information).

The spray head of an electrospray ionization (ESI) source contains a thin, highly charged metal capillary through which the solution to be analyzed is pneumatically forced. The exact position of the capillary tip can often be changed, depending on the source design [1]. The spray head position is adjusted until an optimal intensity is achieved for the species under observation. While generally effective, the lack of a systemic approach exemplifies the need to study and understand how operating parameters, such as spray head position, gas flow rates, and temperature programming, all factor into obtaining high-quality ESI mass spectra.

Electrospray ionization mass spectra can be very sensitive to changes in source conditions, and there are many parameters that can be changed in order to optimize a particular experiment [2]. Electronically, the most significant settings are the capillary voltage and the voltage between skimmer cones, which affect the electric field as the spray head position is adjusted which can have an effect on spray stability [3]. Thermally, the temperature of the source and of the desolvation gas can be independently adjusted over a wide range (typically from ambient to several hundred °C). Volumetrically, the desolvation gas flow rate (as well as any auxiliary gas flows used to enhance desolvation) can be adjusted from tens to hundreds of liters per hour. Spatially, there are often limited adjustments to be made depending on the exact instrument being employed, but generally the position of the spray capillary can be moved in two directions with respect to the skimmer cone (forwards and backwards, side to side), and this position can be optimized against the other parameters.

As experimentalists, we are used to reporting parameters that impact upon the data we collect, but these reported parameters very rarely extend to the physical geometry of the source. Typically, this position is left alone, but is sometimes tweaked to wring
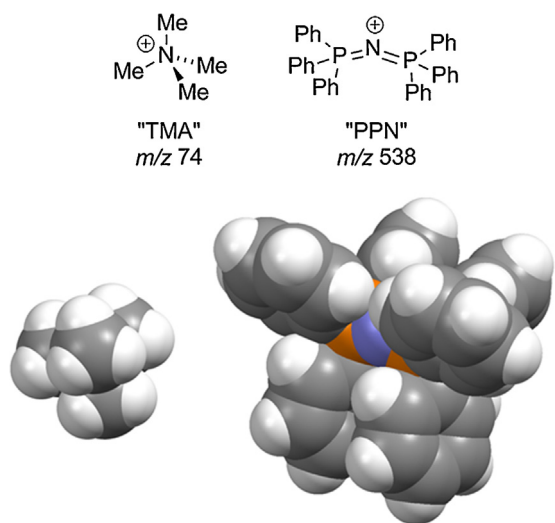
Fig. 1. The two cations investigated in this study. Space-filling models were generated from published crystallographic data files [12].
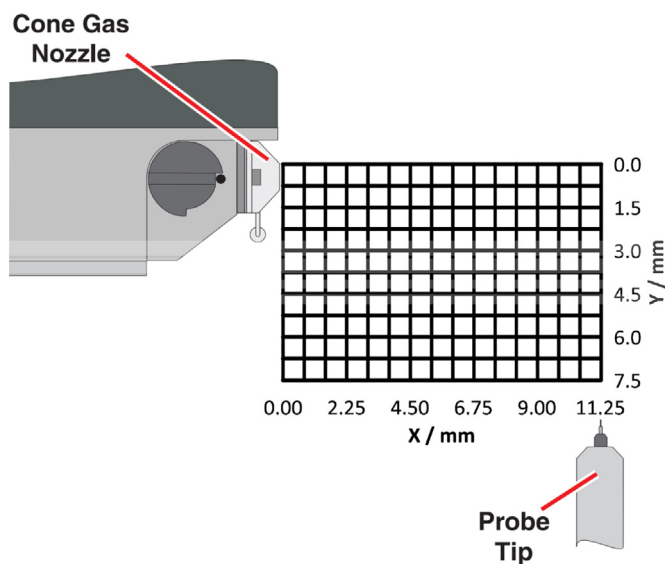

Fig. 2. Illustration of the spray head in its most distant position with respect to the aperture. The grid defines the locations of each analysis. A photo of the ESI source with an overlaid grid may be found in the supporting information (Fig. S15).

out additional performance or perhaps moved more substantially if spray conditions are adjusted. For example, in our own research we use charged tags to "light up" components of a reacting solution and, because these tags have been designed to be highly lipophilic and have non-coordinating counter ions, they are highly surface-active and therefore provide extremely intense spectra even at very low concentrations [4–6]. This highly attractive attribute does have a downside – it limits the upper concentration that can be used, and sometimes we take the step of detuning the instrument to *reduce* the sensitivity. Reducing sensitivity by adjusting the spray head position is a common procedure for ESI-MS; however, the effect this has on analyte response is poorly understood and could end up adversely affecting results if one species becomes substantially overrepresented [7].

We were interested in gaining a more quantitative picture of the effects of spray head position, as we have noticed the often dramatic effect this can have on ion intensity. In particular, we were interested in differential effects, that is, where moving the spray head affected one signal more than another. Electrospray ionization has become increasingly popular as an investigatory tool in the study of reaction mechanisms [8,9] and its explorative capacity may be strengthened with a greater knowledge of instrument response with respect to the position of the capillary spray head, along with other experimentally controlled conditions. In particular, it is important for reproducibility purposes across different concentration ranges that we are not perturbing the relative response of different ions, because such effects may provide misleading kinetic data. Because we mostly use permanently charged ions in our analyses of catalytic reactions by ESI-MS [9–11], we selected two such cations of drastically different mass and shape. $[NMe_4]^+$ is small (m/z 74; tetramethylammonium = TMA) and near-spherical; $[(Ph_3P)_2N]^+$ is large (m/z 538; bis(triphenylphosphine)iminium = PPN) and dumbbell-shaped (Fig. 1).

In polar solvents, the latter is less well solvated and therefore more likely to be found on the outside of a charged droplet, i.e. PPN has higher surface activity and is therefore generally overrepresented in the spectrum [13]. Because the two cations are quaternary ammonium ions (the chloride salt was used in both cases), both are fully dissociated in solution. Sufficiently high concentrations of such salts will cause the observation of aggregates of the form $[(cation)_{n+1}(anion)_n]^+$ in the positive ion mode [14], but these experiments were run at sufficiently low concentration

to avoid appreciable quantities of such aggregate ions. Furthermore, it should be noted that because both compounds are the chloride salt, and m/z 50 is the lower limit of the mass range of our instrument, investigations were carried out in the positive ion mode exclusively.

2. Results and discussion

$[NMe_4]Cl$ and $[(Ph_3P)_2N]Cl$ were mixed in a 1:1 molar ratio, and run at a concentration of $26\,\mu mol\,L^{-1}$. This concentration was chosen after experimenting with a range of values, and this concentration avoided aggregation issues while preserving good intensity across the range of parameters investigated. Rate of infusion can alter relative ion intensities; thus, a constant infusion rate of $10\,\mu L\,min^{-1}$ was employed for all experiments. A full table of experimental conditions is available in the supporting information (Table S1). Additionally, a cross-section diagram of the Q-ToF Micro and Z-Spray source may be found in the supporting information (figure S14). The spray head was rastered across an area 11.25 mm in the y direction and 7.5 mm in the x direction in 0.75 mm increments. Data were collected throughout this process and manipulated in Excel 2013 and OriginPro 9.1 to generate a 3D surface of intensity vs. position for each ion. These contour plots have been color-coded for interpretability such that PPN ion intensity is represented with blue and TMA with green. Scan times were set between 1 and 5 s with an interscan time of 5 s to allow for repositioning of the capillary. Each 3D map involved the collection of 160 unique spectra, and a total of 320 intensity values (one for each of TMA and PPN in each spectrum).

The general response to capillary position was large as anticipated; that is, when the capillary was at its most remote, ion intensity was low, and as the capillary was moved closer, ion intensity increased. This behavior is illustrated in Fig. 2, a contour map of ion intensity of the $[PPN]^+$ and $[NMe_4]^+$ cations vs. capillary tip position, where the x and y values are in millimeters away from the closest possible position to the cone aperture.

It is immediately evident from numerous experiments (see SI figures S1–S13) that there is a large area in which ion intensity is consistently strong, near where the capillary and instrument aperture are closest. When they are most distant, there is a large dead area of little to no intensity. In several experiments, however, the
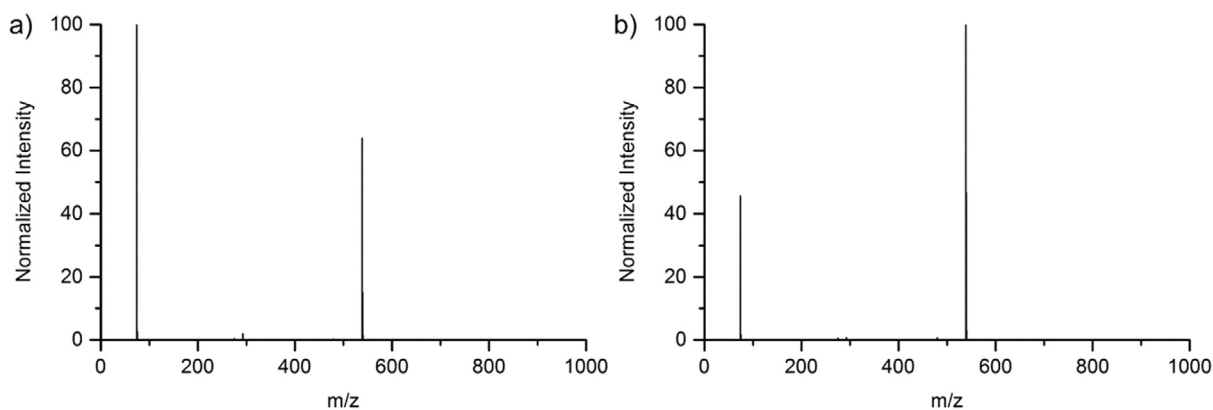
Fig. 3. Mass spectra of 0.0260 mM PPN (m/z 538.2) and TMA (m/z 74.1) in acetonitrile for capillary positions (a) far and (b) near the mass spectrometer aperture.

region of maximum intensity for PPN and TMA was observed at a far y-axis distance but a shallow x-axis distance.

However, closer inspection reveals divergent behavior that becomes obvious when observing instantaneous spectra from the greatest and shortest distance to the mass spectrometer cone in the area sampled (Fig. 3).

A better way of visualizing this is to plot each contour map as a surface in order to observe divergent behavior, or even more plainly, plotting the intensity of the two ions together (Fig. 4). At most cone-capillary distances (shorter distances in particular), the spectrum seems to consist almost entirely of PPN, and the reverse is true at long distances, albeit in a narrower region.

The nature of the two ions gives us a clue in explaining this behavior. TMA, being small and near spherical, has a substantially lower collisional cross section than PPN, and this may be important when ions are being drawn electrostatically into the instrument from long distance. A greater ion mobility may mean it is more efficiently transferred into the mass spectrometer. However, at closer distances, PPN dominates the spectrum, perhaps due to a greater affinity for the surface of the droplet (i.e. a higher surface activity due to it being a bulky and relatively hydrophobic cation).

In a more prosaic sense, the results demonstrate just how sensitive the ESI mass spectrum can be to instrumental settings in cases where the ions are dramatically different in nature. Simply applying a response variation factor to two different ions without ensuring that other parameters are equivalent is a recipe for results that are misleading at best. Given the dramatic differences in response factor that we saw with probe position, we set out to determine if these differences were consistent when we changed other parameters such as solvent, desolvation and cone gas flow rate, and source and desolvation gas temperature.

2.1. Solvent effects

The relationship between surface activity, solvent and ion signal in electrospray has been investigated previously in our group and many others [15–21]; however, the importance of capillary position relative to the sample cone has only limited detail in the literature [22–26]. Zenobi showed that solvent polarity increases when the droplets become smaller at the periphery of the plume or further away from the emitter [27]. Though a great variety of solvents and ESI source arrangements have been utilized, the relationship of these two parameters together has not been rigorously investigated [1,28–30]. Our investigations using multiple solvents clearly demonstrate that capillary position is an important factor in ion selectivity. The effect on ion intensity from one solvent to another can be dramatic and should be taken into account for any quantitative experiments.

Running the experiment in methanol instead of acetonitrile led to almost complete suppression of the TMA signal by PPN, by a factor of greater than 1500:1 across the entire area examined (Fig. 5). In fact, the only region where TMA had any appreciable intensity at all was when the capillary was near the cone in the x direction, but far from it in the y direction. This increased ion segregation is presumably a function of the enhanced solvation of TMA vs. PPN in methanol, leaving the PPN to occupy the surface sites of the droplets and over-representing the PPN ions accordingly. "Offspring droplets" are thought to carry disproportionate quantities of the excess charge (~15%) compared to the total mass (~2%) of their precursors [13,31], and hence we may expect that sampling the plume at distance may increase the amount of the most surface-active ion observed.

Spectra collected from water displayed behavior similar to methanol, with PPN dominating the spectrum nearly everywhere, but the regions of high intensity were even more localized (Fig. 6). The dead zone for PPN was large, and extended into the area where the capillary was close to the cone. This behavior is almost certainly a function of the fact that the desolvation conditions were not optimized for water, and the degree of droplet desolvation was likely insufficient at shorter distances. Buildup of water on the
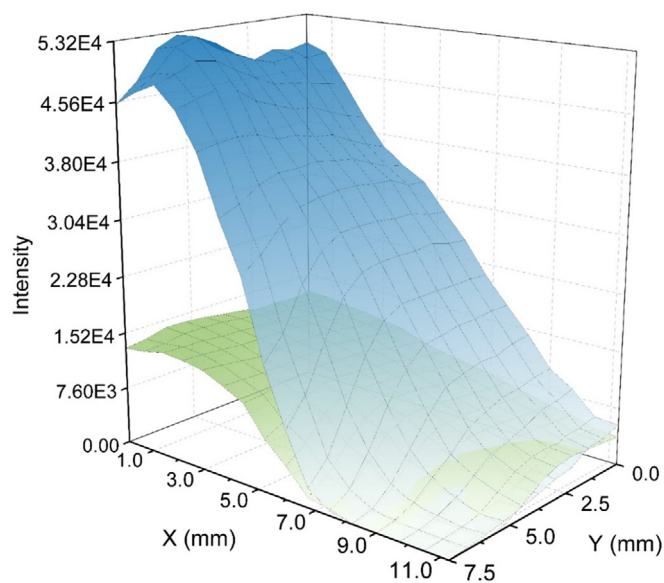

Fig. 4. Overlaid ESI-MS intensities of an equimolar mixture of PPN and TMA at varying capillary positions. Note the divergent behavior far from the MS aperture. Refer to Table S1, experiment 4, in supporting information for experiment parameters.
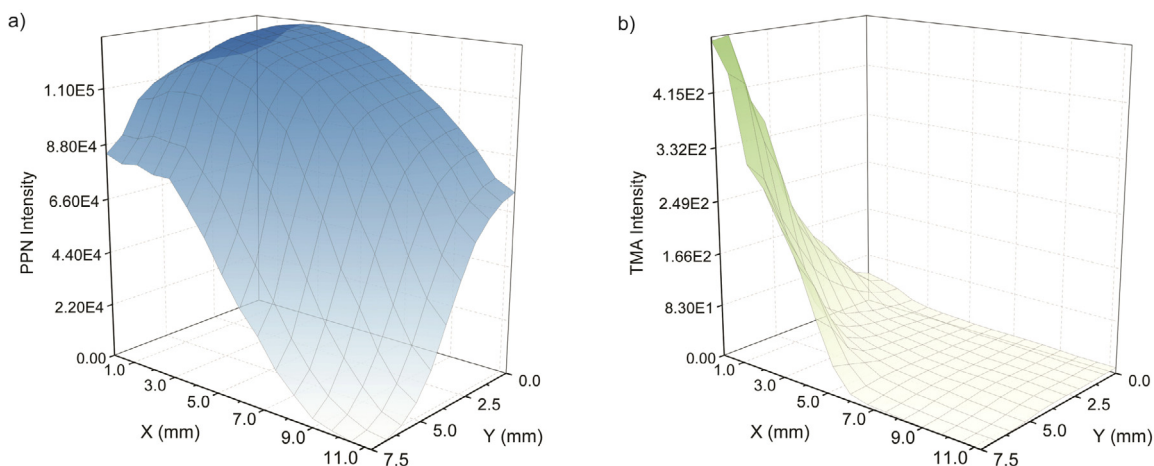
Fig. 5. Intensity vs. capillary position for (a) PPN vs. (b) TMA in methanol. Note the difference in the vertical axes in the two plots (0–150,000 vs. 0–500). Refer to Table S1, experiment 5, in supporting information for experiment parameters.
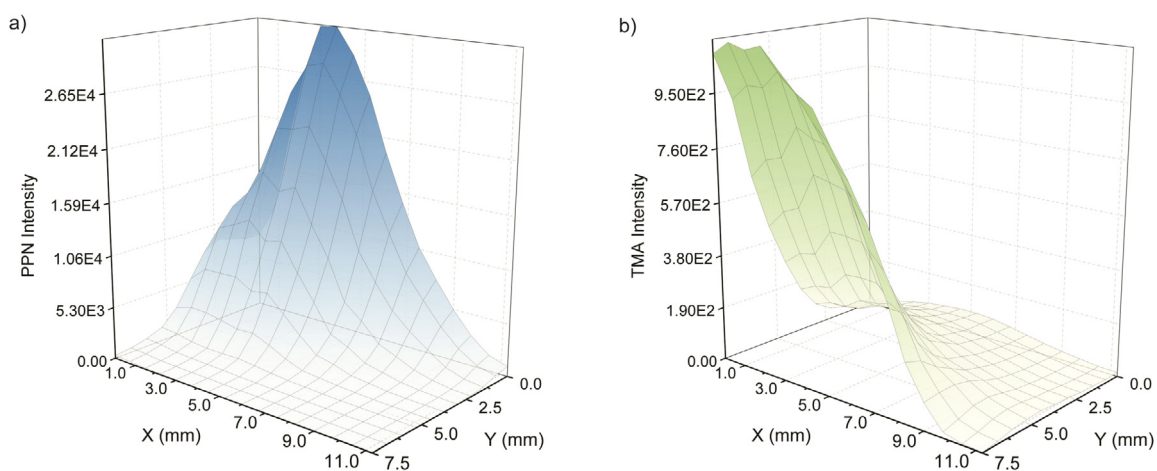

Fig. 6. Intensity vs. capillary position for (a) PPN vs. (b) TMA in water. Note the orders-of-magnitude difference in the vertical axes in the two plots. Refer to Table S1, experiment 11, in supporting information for experiment parameters.

baffle opposite the capillary is evidence for insufficiently vigorous desolvation conditions.

The nature of the electrospray process supports the differences observed between solvents. The nebulization of solvent droplets with high charge density promotes liberation of highly mobile ions from the droplets. As a result of the differential ion mobility between PPN and TMA, one ion may be given preference for desolvation and appear relatively over-represented [31–36]. PPN overwhelmingly dominates in most solvents, indicative of the high surface activity of the bulky ion. In spite of this, optimal positioning of the capillary is a key factor as evidenced by the poor desolvation of PPN in much of the 2D plane when in water. Due to these discrepancies, movement of the spray head outside of the "sweet spot" during analysis could lead to substantial quantitative error.

2.2. Gas flow rates

The cone gas and desolvation gas flow rates may be adjusted across a wide range and are known to alter the response of the instrument. With this in mind, the experiment was performed with varying nitrogen gas flow rates. The sample cones (or skimmer cones) are in place to provide a smooth transition between the atmospheric pressure of the ESI source and the high vacuum of the mass analyser. While the sample cone is set perpendicular to the spray capillary to avoid contamination, a flow of nitrogen gas

is required for added protection of the cone and may be manually adjusted by the operator. The cone gas flow rate varies based on a variety of factors, but it is generally set between 100 and 300 L h^{-1}. Plots were collected with low cone gas flow rates of 100 and 50 L h^{-1} for the sake of comparison. As seen in Fig. 7(a and b), the difference in flow rates was observed to have minimal effect on the intensities of either of the two ions across the area sampled. Both plots for 50 and 100 L h^{-1} cone gas flow rate show similar profiles and intensity across the entire area plane, suggesting a higher flow rate may be an unnecessary strain on gas reserves unless solvent adducts or cluster ions are observed.

Conversely, dramatic changes are observed for changes to the desolvation gas (Fig. 8). Desolvation gas is the heated nitrogen flowing over the stream of droplets produced by the source to assist in desolvation of analyte ions. Adjustment of the desolvation gas has a large effect on the response of each ion, which clearly demonstrates the importance of desolvation gas flow rate in facilitating the transfer of ions to the gas phase.

Flow rates of 50–200 L h^{-1} provided very similar results, but at 25 L h^{-1} the intensity of PPN dropped off considerably, suggesting inadequate desolvation, except perhaps near the center of the plume (i.e. where the capillary is close to the cone). The increase in intensity near (0, 0) for the lowest gas flow rate is very likely due to the increase in field strength as the capillary approaches the MS aperture. Predominantly, the results obtained
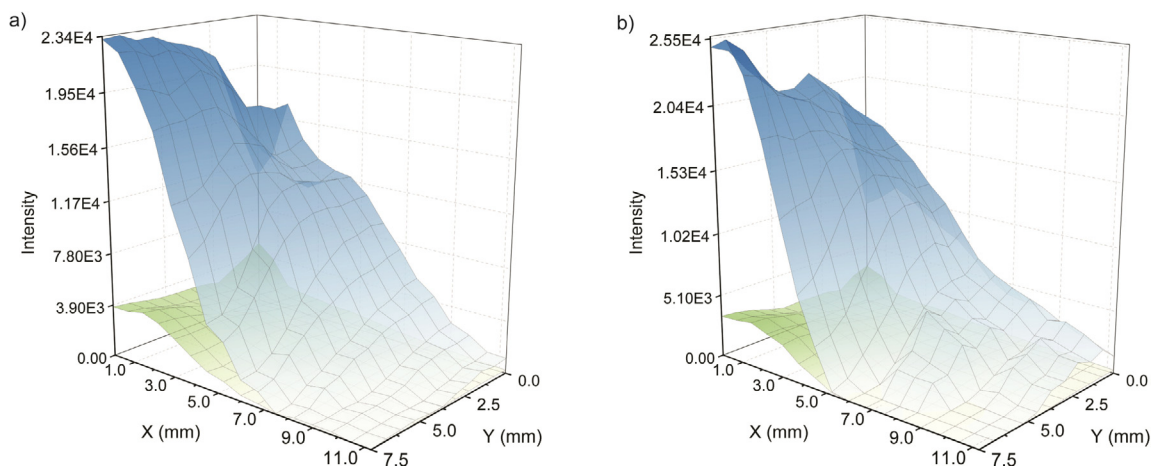
Fig. 7. PPN (above) and TMA (below) ion intensity at 0.260 mM in MeCN with (a) 50 L h^{-1} cone gas flow rate and (b) 100 L h^{-1}. Refer to Table S1, experiments 2 and 3, in supporting information for experiment parameters.
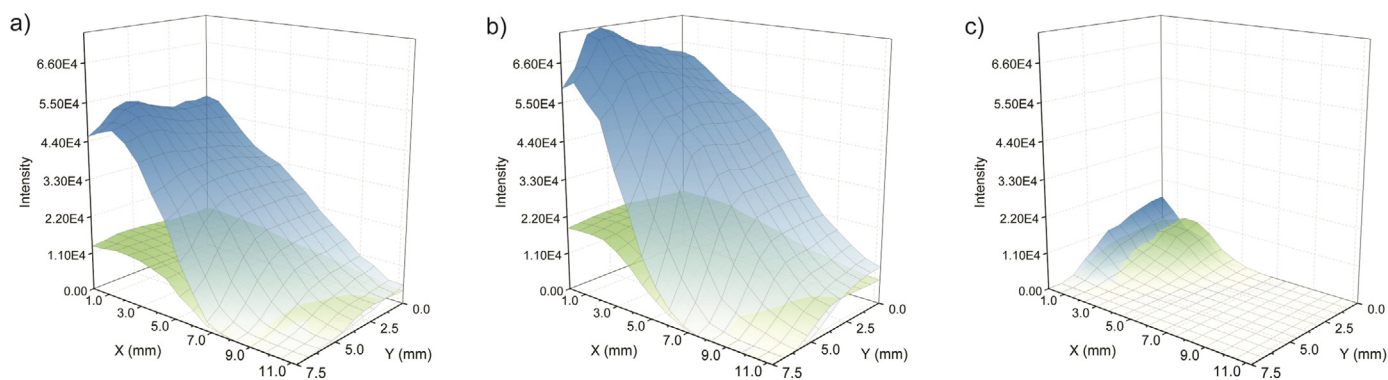

Fig. 8. PPN and TMA ion intensity at 26 μM in MeCN with (a) 200 L h^{-1} desolvation gas flow rate, (b) 50 L h^{-1} and (c) 25 L h^{-1}. Refer to Table S1, experiments 4, 6 and 8, in supporting information for experiment parameters.

for changes to the desolvation gas flow rate are intuitive and do not contribute appreciably to differential response. As expected, either ion has a distinct range in which its response is maximized which may be exploited depending on the nature of the analyte. Unwanted suppression of an analyte could be minimized by adjusting not only the capillary position, but also the desolvation gas flow rate.

2.3. Temperature programming

Temperature programming for the average electrospray ionization source setup involves two parts of the ESI source: the probe (usually referred to as the "source temperature") and the warmed inert bath-gas (the "desolvation temperature"). ESI-MS temperature programming effects have been studied in some detail, though not spatially. Previous studies have demonstrated the importance of temperature programming and the potentially profound implications temperature has on the electrospray process [37,38]. Temperature has been shown to have considerable effects in ion mobility ESI-MS by facilitating desolvation or causing potential issues in the thermal denaturation of proteins upon analysis [39,40]. Source and desolvation temperature are independently controlled and they affect the transfer of solvated analytes to desolvated ions in different ways; therefore, the effects of each will be discussed separately.

2.4. Source temperature

The temperature of the source is generally set around the boiling point of the solvent used (or higher) in order to promote desolvation. For example, analysis of aqueous solutions would necessitate the source temperature to be set to 100 °C or more to promote solvent evaporation. Three source temperatures were studied using the same equimolar mixture of PPN in acetonitrile (b.p. 82 °C) for adequate contrast: slightly above the boiling point at 89 °C, 39 °C, and 150 °C. In these three trials, the desolvation temperature was held constant at 189 °C.

Variation in source temperature had an effect very similar to that of variations in desolvation gas flow rate. That is, lowered temperatures led to appreciable ion counts only when the capillary was close to the aperture (Fig. 9). An increase in source temperature promotes desolvation and thus signal intensity. Furthermore, the increased source temperature vastly improves analyte response over the majority of the capillary plane when compared to a lower source temperature. A wide region of high-intensity signal that appears at high temperature is shared by both PPN and TMA. At lowered temperature, the signal for TMA is much more sharp and localized close to the source. In comparison, the signal for TMA at the same (lowered) temperature is relatively localized to the source (compared to the signal) but is also much broader. This is a testament to how small and highly mobile ions, such as TMA, are
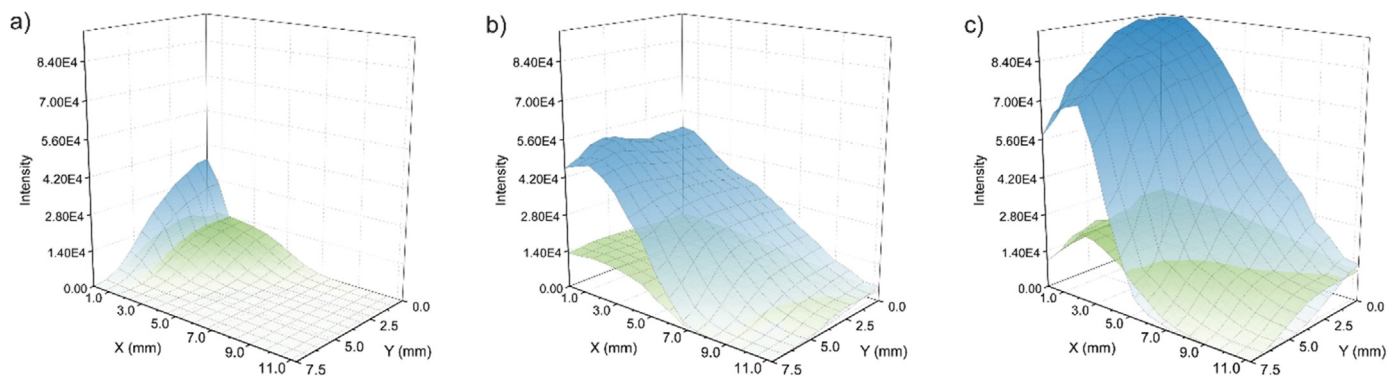
Fig. 9. PPN and TMA ion intensity at 26 μM in MeCN with a source temperature of (a) 39 °C, (b) 89 °C, and (c) 150 °C. Refer to Table S1, experiments 4, 10, and 13, in supporting information for experiment parameters.

readily evaporated from the electrospray plume even at reduced temperatures. Notably, the increase in temperature from 89 °C to 150 °C gave rise to only minor changes in the contour plots for both PPN and TMA. Maximum intensity remained relatively constant between trials, though high signal intensity persisted for greater "y" distances from the MS aperture at a source temperature of 89 °C than at an elevated temperature of 150 °C (Fig. 9). This indicates that attempting to gain greater sensitivity by adjusting the source temperature high above a solvent's boiling point is not necessary unless the ions are particularly difficult to liberate from the solvent (not the case here for these hydrophobic ions, but definitely an issue for more highly functionalized molecules such as peptides). Instead, source temperature should be held slightly above the boiling point while other parameters are adjusted.

2.5. Desolvation temperature

In the investigation of desolvation temperature effects the source temperature was held constant at the boiling point of the solvent used. Instrument response seemed quite insensitive to desolvation gas temperature – the contour plots for both 89 °C and 189 °C are very similar in terms of overall shape and intensity (Fig. 10). These results suggest the warm bath gas temperature is not as important as other parameters in tuning signal intensity. As seen in Fig. 10, a 100 °C decrease in desolvation temperature produces little difference in maximum intensity for both PPN and TMA. However, the profiles of both ions at differing desolvation temperature are somewhat interesting. There is clearly an elongated area of sensitivity stretching away from the MS aperture. It seems that the decrease in desolvation gas temperature yields a more particular profile in which larger "y" distances become more accessible, though the favorable "x" positioning is narrowed perpendicular to the aperture. The higher temperature seems to preserve the surface activity advantage of PPN across a wider range of distances. At the lower temperature and furthest extents, TMA is relatively competitive with PPN, as seen by the divergent behavior in Fig. 10. This is probably due to the fact the smaller ion has higher mobility and hence is more efficiently transported across the long distance from capillary to aperture.

2.6. Experimental

Solvents and chemicals were purchased from Sigma-Aldrich. Anhydrous and air-free acetonitrile and methanol were purified with an MBraun solvent purification system before use. Deionized water was obtained from a Millipore Milli-DI water purification system. Equimolar 100 mL solutions of

bis(triphenylphosphine)iminium chloride and tetramethylammonium chloride were separately prepared in a variety of solvents at a concentration of 26 μmol L^{-1}. This solution was fed into the ESI source through the use of a syringe pump and a Hamilton GasTight analytical syringe connected to a fixed length of PEEK tubing. The flow rate was set to 10 μL min^{-1} for all experiments. Prior to each run, instrument cleanliness and stability were ensured through rinsing with the appropriate solvent and acquisition of stable analyte signal from the subsequent sample solution. After achieving a steady signal the spray head was moved to a known position, furthest from the mass spectrometer aperture. Data points were acquired with 1–5 s of scan time and 1–5 s of interscan time. The relatively high scan and interscan times ensured that high quality data were obtained and plenty of time was allotted for smooth movement of the spray head to each desired position in the xy plane. Movement in the xy plane was tracked by markers affixed to the ESI probe adjustment collars, corresponding to a distance of 0.75 mm in the x-direction and 0.75 mm in the y-direction. Several runs were repeated in the forward and reverse direction, and then compared to ensure reproducibility of the data acquired. Furthermore, the experiment was found to have excellent reproducibility through the comparison of several trials performed with the same experimental parameters. Data analysis was assisted by Chemcalc.org [41].

2.7. Instrument parameters

All electrospray ionization mass spectra were collected in the positive ion mode on a Waters Micromass Q-TOF Micro mass spectrometer. While many settings were adjusted throughout the course of the experiments, the following parameters were left constant throughout. The capillary voltage was held at 2.9 kV, cone voltage at 15.0 V, and extraction cone at 0.5 V. The collision energy was left quite low at 2.0 V since the intrinsic charge of the analytes used effected an excellent signal. The MCP detector on the instrument was set to 2.7 kV. Most other parameters varied according to what was being investigated during that particular experiment. Inter-scan time varied according to the operator's preference, as each operator may require more or less time to reach the desired acquisition point. Accordingly, inter-scan time is not expected to have any effect on data acquisition. Several trials were run with similar conditions and combined to form an average of several runs. In the event that the scan time differed, the runs were weighted based on scan time before averaging. Once completed the data from the run was extracted through selected ion monitoring (SIM) of m/z 538.2 for PPN and m/z 74.1 for TMA and was subsequently plotted by relating
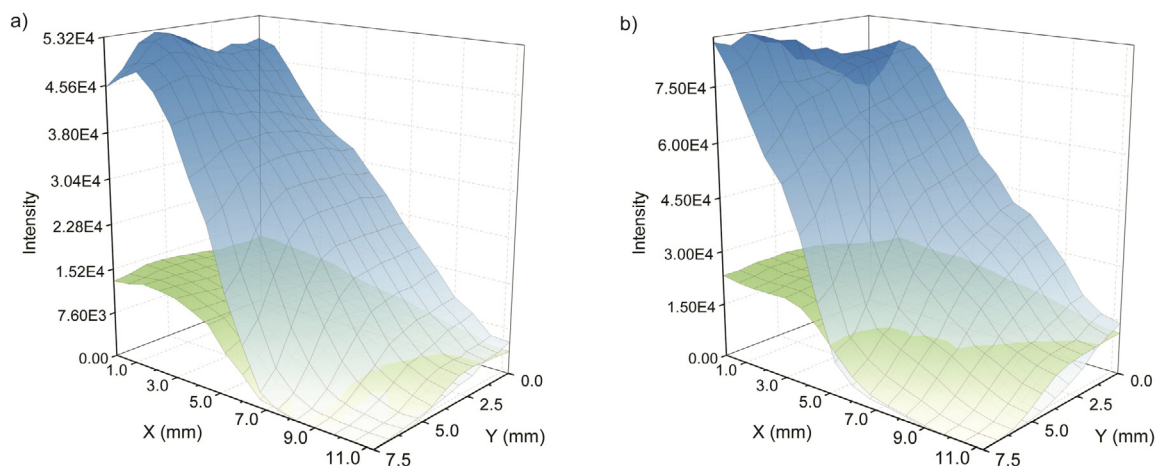
Fig. 10. PPN and TMA ion intensity at 26 μM in MeCN with a desolvation temperature of (a) 189 °C and (b) 89 °C. Refer to Table S1, experiments 4, 10, and 13, in supporting information for experiment parameters.

the acquisition time of individual points to the position of the spray-head.

3. Conclusions

The relative and absolute ion abundances of PPN and TMA cations were examined with respect to capillary position for a range of common experimental parameters for ESI-MS. In general, the evidence obtained suggests variation in the x-axis distance between the MS aperture and the spray head has a greater impact on signal intensity than do changes in the y-axis. Discrepancies in ESI-MS response to different analytes is a well-known phenomenon, which can be affected greatly by experimental conditions as evidenced by the data collected.

However, the geometry of the source not only affects the overall sensitivity of the technique, but in extreme cases, the relative response of two ions can even reverse. It is important to keep this divergent behavior in mind when implementing ESI-MS due to the great deal of tunable parameters, variations in sample preparation, source geometries and designs, and supplementary variables associated with ESI-MS analysis.

Acknowledgements

Appendix A. Supplementary data

Supplementary material related to this article can be found, in the online version, at http://dx.doi.org/10.1016/j.ijms.2015.07.016

References

[1] H. Stahnke, S. Kittlaus, G. Kempe, C. Hemmerling, L. Alder, The influence of electrospray ion source design on matrix effects, J. Mass Spectrom. 47 (2012) 875–884.

[2] P. Kebarle, U.H. Verkerk, Electrospray: from ions in solution to ions in the gas phase, what we know now, Mass Spectrom. Rev. 28 (2009) 898–917.

[3] L. Parvin, M.C. Galicia, J.M. Gauntt, L.M. Carney, A.B. Nguyen, E. Park, L. Heffernan, A. Vertes, Electrospray diagnostics by Fourier analysis of current oscillations and fast imaging, Anal. Chem. 77 (2005) 3908–3915.

[4] M.A. Henderson, J. Luo, A. Oliver, J.S. McIndoe, The Pauson-Khand reaction: a gas-phase and solution-phase examination using electrospray ionization mass spectrometry, Organometallics 30 (2011) 5471–5479.

[5] Z. Ahmadi, C.C. Manning, D.A. Harrington, J.S. McIndoe, Powerful insight into catalytic mechanisms through simultaneous monitoring of reactants, products, and intermediates, Angew. Chem. Int. Ed. 50 (2011) 8304–8306.

[6] Z. Ahmadi, A.G. Oliver, J.S. McIndoe, An unexpected pathway for ligand substitution in an aryl halide complex of palladium, Chempluschem 78 (2013) 632–635.

[7] K. Hiraoka, K. Murata, I. Kudaka, Species-selectivity effects in the production of electrospray ions, Rapid Commun. Mass Spectrom. 7 (1993) 363–373.

[8] K. Vikse, T. Naka, J.S. McIndoe, M. Besora, F. Maseras, Oxidative additions of aryl halides to palladium proceed through the monoligated complex, ChemCatChem 5 (2013) 3604–3609.

[9] J. Luo, A.G. Oliver, J.S. McIndoe, A detailed kinetic analysis of rhodium-catalyzed alkyne hydrogenation, Dalton Trans. 42 (2013) 11312–11318.

[10] Z. Ahmadi, J.S. McIndoe, A mechanistic investigation of hydrodehalogenation using ESI-MS, Chem. Commun. (Camb). 49 (2013) 11488–11490.

[11] K.L. Vikse, Z. Ahmadi, J. Scott McIndoe, The application of electrospray ionization mass spectrometry to homogeneous catalysis, Coord. Chem. Rev. 279 (2014) 96–114.

[12] D.J. Evans, D.L. Hughes, Structure of tetramethylammonium bromide: a redetermination, Acta Crystallogr. Sect. C Cryst. Struct. Commun. 46 (1990) 1452–1454.

[13] P. Kebarle, M. Peschke, On the mechanisms by which the charged droplets produced by electrospray lead to gas phase ions, Anal. Chim. Acta 406 (2000) 11–35.

[14] P.J. Dyson, J.S. McIndoe, D. Zhao, Direct analysis of catalysts immobilised in ionic liquids using electrospray ionisation ion trap mass spectrometry, Chem. Commun. (2003) 508–509.

[15] A.P. Bruins, Mechanistic aspects of electrospray ionization, J. Chromatogr. A 794 (1998) 345–357.

[16] N.B. Cech, C.G. Enke, Selectivity in electrospray ionization mass spectrometry, in: Electrospray and MALDI Mass Spectrometry, John Wiley & Sons, Inc., 2010, pp. 49–73.

[17] J. Li, J.A. Taraszka, A.E. Counterman, D.E. Clemmer, Jianwei Li, A. John, Taraszka, E. Anne, D.E.C. Counterman, Influence of solvent composition and capillary temperature on the conformations of electrosprayed ions: unfolding of compact ubiquitin conformers from pseudonative and denatured solutions, Int. J. Mass Spectrom. 185 (1998) 37–47.

[18] M.A.H. Amad, N.B. Cech, G.S. Jackson, C.G. Enke, Importance of gas-phase proton affinities in determining the electrospray ionization response for analytes and solvents, J. Mass Spectrom. 35 (7) (2000) 784–789.

[19] J.M.E. Quirke, Y.-L. Hsu, G.J. Van Berkel, Ferrocene-based electroactive derivatizing reagents for the rapid selective screening of alcohols and phenols in natural product mixtures using electrospray-tandem mass spectrometry, J. Nat. Prod. 63 (2000) 230–237.

[20] L. Konermann, E. Ahadi, A.D. Rodriguez, S. Vahidi, Unraveling the mechanism of electrospray ionization, Anal. Chem. 85 (2013) 2–9.

[21] J. Pape, K.L. Vikse, E. Janusson, N. Taylor, J.S. McIndoe, Solvent effects on surface activity of aggregate ions in electrospray ionization, Int. J. Mass Spectrom. 373 (2014) 66–71.

[22] I. Manisali, D.D.Y. Chen, B.B. Schneider, Electrospray ionization source geometry for mass spectrometry: past, present, and future, TrAC Trends Anal. Chem. 25 (2006) 243–256.

[23] A.P. Bruins, T.R. Covey, J.D. Henion, Ion spray interface for combined liquid chromatography/atmospheric pressure ionization mass spectrometry, Anal. Chem. 59 (1987) 2642–2646.

[24] J.S. Page, R.T. Kelly, K. Tang, R.D. Smith, Ionization and transmission efficiency in an electrospray ionization-mass spectrometry interface, J. Am. Soc. Mass Spectrom. 18 (2007) 1582–1590.

[25] K. Benkestock, G. Sundqvist, P.-O. Edlund, J. Roeraade, Influence of droplet size, capillary-cone distance and selected instrumental parameters for the analysis of noncovalent protein-ligand complexes by nano-electrospray ionization mass spectrometry, J. Mass Spectrom. 39 (2004) 1059–1067.

[26] K. Tang, J.S. Page, R.D. Smith, Charge competition and the linear dynamic range of detection in electrospray ionization mass spectrometry, J. Am. Soc. Mass Spectrom. 15 (2004) 1416–1423.

[27] R. Wang, R. Zenobi, Evolution of the solvent polarity in an electrospray plume, J. Am. Soc. Mass Spectrom. 21 (2010) 378–385.

[28] M. Ikonomou, A. Blades, P. Kebarle, Investigations of the electrospray interface for liquid chromatography/mass spectrometry, Anal. Chem. (1990) 957–967.

[29] E.J. Maxwell, D.D.Y. Chen, Twenty years of interface development for capillary electrophoresis-electrospray ionization-mass spectrometry, Anal. Chim. Acta 627 (2008) 25–33.

[30] R.B. Cole, A.K. Harrata, Solvent effect on analyte charge state, signal intensity, and stability in negative ion electrospray mass spectrometry; implications for the mechanism of negative ion formation, J. Am. Soc. Mass Spectrom. 4 (1993) 546–556.

[31] L. Tang, P. Kebarle, Dependence of ion intensity in electrospray mass spectrometry on the concentration of the analytes in the electrosprayed solution, Anal. Chem. 65 (1993) 3654–3668.

[32] N.B. Cech, C.G. Enke, Practical implications of some recent studies in electrospray ionization fundamentals, Mass Spectrom. Rev. 20 (2002) 362–387.

[33] P. Kebarle, A brief overview of the present status of the mechanisms involved in electrospray mass spectrometry, J. Mass Spectrom. 35 (2000) 804–817.

[34] C.G. Enke, A predictive model for matrix and analyte effects in electrospray ionization of singly-charged ionic analytes, Anal. Chem. 69 (1997) 4885–4893.

[35] N.B. Cech, C.G. Enke, Relating electrospray ionization response to nonpolar character of small peptides, Anal. Chem. 72 (2000) 2717–2723.

[36] T.L. Constantopoulos, G.S. Jackson, C.G. Enke, Effects of salt concentration on analyte response using electrospray ionization mass spectrometry, J. Am. Soc. Mass Spectrom. 10 (1999) 625–634.

[37] H. Murata, T. Takao, Y. Shimonishi, T. Matsuo, Optimization of skimmer voltages of an electrospray ion source coupled with a magnetic sector instrument, Rapid Commun. Mass Spectrom. 8 (1994) 205–210.

[38] J.S. Page, I. Marginean, E.S. Baker, R.T. Kelly, K. Tang, R.D. Smith, Biases in ion transmission through an electrospray ionization-mass spectrometry capillary inlet, J. Am. Soc. Mass Spectrom. 20 (2009) 2265–2272.

[39] Y.H. Chen, H.H. Hill Jr., D.P. Wittmer, Thermal effects on electrospray ionization ion mobility spectrometry, Int. J. Mass Spectrom. Ion Process. 154 (1996) 1–13.

[40] U.A. Mirza, S.L. Cohen, B.T. Chait, Heat-induced conformational changes in proteins studied by electrospray ionization mass spectrometry, Anal. Chem. 65 (1993) 1–6.

[41] L. Patiny, A. Borel, ChemCalc: a building block for tomorrow's chemical infrastructure, J. Chem. Inf. Model. 53 (2013) 1223–1228.